Available online at www.sciencedirect.com

ScienceDirect

IFAC PapersOnline CONFERENCE PAPER ARCHIVE

IFAC PapersOnLine 54-2 (2021) 19–24

H_∞ State Feedback Controller for ODE Model of Traffic Flow

Mehmet Ali Silgu [*,**,***] **İsmet Gökşad Erdağı** [*,**] **Gökhan Göksu** [*] **Hilmi Berk Çelikoğlu** [*,**]

[*] *Intelligent Transportation Systems Research Lab, Istanbul Technical University (ITU), 34469, Istanbul, Turkey (e-mails: {msilgu,erdagi,goksug,celikoglu}@itu.edu.tr).*

[**] *Department of Civil Engineering, Istanbul Technical University (ITU), 34469, Istanbul, Turkey*

[***] *Department of Civil Engineering, Bartin University, 74100, Bartin, Turkey (e-mail: masilgu@bartin.edu.tr)*

Abstract: In this study, we propose an H_∞ state feedback controller for freeway traffic flow. The integrated freeway traffic flow management scheme is applied through coordination of ramp metering and variable speed limit. In order to improve the service characteristics of mainstream and on-ramps, we have designed a controller that sustains the mainstream flow around a critical density while concerning the on-ramp queue lengths. We have used the state space discretized ODE model of traffic flow to design continuous-time feedback controllers. The performance of the controller is validated on a micro-simulation environment which is calibrated by field data. The simulation results show that the H_∞ controller decreases the average densities and the average queue lengths on on-ramps.

Keywords: Traffic modelling and control, H_∞ control, ramp metering, variable speed limit

1. INTRODUCTION

One of the major goals of freeway traffic management is to maximize throughput without constructing new infrastructures such as additional lanes or new roads. Prior to field implementation, it is a common practice to test control and operational strategies by simulation Celikoglu and Dell'Orco (2008); Müller et al. (2015); Fountoulakis et al. (2017); Sadat and Celikoglu (2017); Silgu et al. (2018).

Ramp metering (RM) and variable speed limit (VSL) have been designed with various goals including feedback control Carlson et al. (2011, 2014); Iordanidou et al. (2015), robust control Hajiahmadi et al. (2013, 2016), multi-objective control Luspay et al. (2017), proportional-integral control Pasquale et al. (2014) and optimal control Gomes and Horowitz (2006); Caligaris et al. (2007); Roncoli et al. (2015a,b). The studies Lu et al. (2010a) and Lu et al. (2010b), RM and VSL are applied in order to maximize the throughput of a recurrent bottleneck. Stability analysis of VSL control is analyzed in Zhang and Ioannou (2018a,b) A model predictive control based feedback controller and a feedforward controller are applied in order to prevent shockwave propagation in Csikós et al. (2013).

H_∞ control is a powerful tool in analysing the stability of nonlinear systems under bounded disturbances. The methods of H_∞ restricts the effects of exogenous disturbances on the dynamical system behavior up to an H_∞ gain. Traffic flow as a dynamical system, there are applications analyzing the stability of traffic state under disturbances with H_∞ control methodologies Lemarchand et al. (2011); Mohajerpoor et al. (2020). However, H_∞ control approaches have not been considered for ensuring the stability of the mainstream density of a freeway and the queue lengths of the on-ramps under flow disturbances to the mainstream and on-ramps.

The main contributions of this work can be summarized as follows:

- An H_∞ state feedback controller (H_∞ SFC) is designed in order to regulate the mainstream and to keep at a critical density.
- While keeping the mainstream density at critical level, the queue lengths of the on-ramps are also taken into account to avoid spillback.
- The H_∞ SFC is proposed to ensure the asymptotic stability of the closed-loop system and to meet an H_∞ gain and performance for disturbances coming to the on-ramps and to the beginning of the mainstream.
- The state feedback controller has been tested to regulate traffic flow on a the real freeway network piece, which is simulated using real data on a micro-simulation environment.

In this study, we propose a novel controller for the integrated control of freeway traffic. We have designed an H_∞ state-feedback controller (H_∞ SFC) to regulate the freeway mainstream by keeping the flow at a critical density while taking into account the queue dynamics using RM and VSL techniques. On purpose we have adopted the ordinary differential equations (ODE) model of Lighthill-Whitham-Richards (LWR) (see Chapter 9 of Kachroo and Ozbay (2003) for single input case). Seeking the control of the disturbances due to the on-ramp inflows with a controlled output, the H_∞ SFC we have proposed ultimately aims to suppress the system disturbances. We are not aware of such a controller as described and differentiated above. We have sought the validation and the performance of

10.1016/j.ifacol.2021.06.003

the controller we propose over a micro-simulation environment, in which we calibrate the simulation model using field data from a real case involving multiple on-ramps and a single off-ramp.

The organization of the paper is as follows: In the beginning, we provide a standard notation, the basic definitions, and lemmas. We describe and state our problem in Section III. We define the H_∞ state feedback controller in Section IV. In Section V, we introduce the real freeway test field where we integrate the proposed controller using micro-simulation. We discuss the simulation results in Section VI and conclude with concluding remarks and future research in the final section.

2. BASIC DEFINITIONS AND LEMMAS

We adopt the standard notation among the paper. Inside the matrix blocks, "*" stands for the corresponding conjugate term or block of the upper triangular matrix. C^0, C^1 and L_2 denote the continuous function, continuously differentiable function classes on their domain of existence and the square integrable function class, respectively. We assume that all the matrices are compatible for algebraic operations. Given vectors $\mathbf{x}_1$ and $\mathbf{x}_2$ with appropriate dimensions and a positive definite symmetric matrix P, $\mathbf{x}_1^T P\mathbf{x}_2 + \mathbf{x}_2^T P\mathbf{x}_1$ is expressed as $2\mathbf{x}_1^T P\mathbf{x}_2$, for simplicity.

Let us consider a nonlinear system

$$\dot{\mathbf{x}}(t) = f(\mathbf{x}(t)), \quad \mathbf{x}(0) = \mathbf{x}_0 \tag{1}$$

where $\mathbf{x}(t) \in \mathscr{D} \subseteq \mathbf{R}^n$ is the state vector. Here, the sufficiently smooth vector field $f \in C^0$ defined as $f : \mathscr{D} \to \mathbf{R}$. If $f(\mathbf{x}_e) = 0$, then the point $\mathbf{x}_e \in \mathscr{D}$ is said to be the equilibrium point of the operating system. For ease of notation, we will state all definitions and theorems for $\mathbf{x}_e = 0$. In order to present the main result of the paper, we need the following stability definitions (Khalil, 2002, Definition 4.1.).

Definition 1. The equilibrium point of the system (1) is said to be stable, if for every $\varepsilon > 0$, there exists a $\delta > 0$ such that, $\|\mathbf{x}_0\| < \delta$ implies $\|\mathbf{x}(t)\| < \varepsilon$, for every $t \geq 0$.

Definition 2. The equilibrium point of the system (1) is said to be asymptotically stable, if it is stable and there exists $\delta > 0$ such that, $\|\mathbf{x}_0\| < \delta$ implies $\lim_{t\to\infty} \|\mathbf{x}(t)\| = 0$.

Definition 3. A continuous scalar function $V : \mathbf{R}^n \to \mathbf{R}$ is said to be Lyapunov function if for any $R_\varepsilon > 0$

- $V(\mathbf{0}) = 0$ and
- $V(\mathbf{x}) > 0$, $\forall \mathbf{x} \in B_\varepsilon = \{\mathbf{x} \mid \|\mathbf{x}\| < R_\varepsilon\} - \{\mathbf{0}\}$,

holds.

Theorem 4. The dynamical system (1) is locally asymptotically stable, if there exists a Lyapunov function $V(\mathbf{x})$ satisfying

$$\dot{V} = \frac{dV(\mathbf{x})}{dt} = \nabla V \cdot f(\mathbf{x}(t)) < 0, \tag{2}$$

$\forall \mathbf{x} \in B_\varepsilon = \{\mathbf{x} \mid \|\mathbf{x}\| < R_\varepsilon\} - \{\mathbf{0}\}$.

Remark 1. The dynamical system (1) is globally asymptotically stable, if there exists a Lyapunov function $V(\mathbf{x})$ satisfying (3) for all $\mathbf{x} \in \mathbf{R}^n - \{\mathbf{0}\}$.

Lemma 5. (Boyd and Vandenberghe (2004)). Let A, B, C be constant matrices with compatible dimensions satisfying $A = A^T$ and $C = C^T$ and $C > 0$. Then, the LMI $X = \begin{bmatrix} A & B \\ * & -C \end{bmatrix} < 0$ is equivalent to $A + BC^{-1}B^T < 0$.

3. PROBLEM STATEMENT

We formulate the problem of integrated RM and VSL control considering an actual freeway corridor that is composed of the mainline with multiple on-ramps and a single off-ramp, as shown by Figure 1.

The variables, which are used in Figure 1, used to formulate the equations to represent the flow dynamics for this problem are presented as follows:

- $\rho_i(t)$ is the density on the i^{th} segment of the road at time t,
- $q(x,t)$ denotes the flow of the road at distance x and time t,
- $u_{VSL}(t)$ represents the flow to be controlled via VSL of the road at distance $x = 0$ and time t,
- $u_{RM,i}(t)$ symbolizes the flow to be controlled via RM for the i^{th} ramp at time t and
- $q_{out,i}(t)$ expresses the flow for the i^{th} off-ramp at time t.
- $r_i(t)$ exemplifies the number of vehicles entering the i^{th} ramp at time t.
- $l_i(t)$ typifies the queue length of the ramp entering into the Segment i at time t.

From the ODE model of traffic flow, we have

$$\begin{aligned} \dot{\rho}_1(t) &= \frac{u_{VSL}(t) - q(L_1^-,t)}{L_1}, \\ \dot{\rho}_{k+1}(t) &= \frac{q(L_k^+,t) - q(L_{k+1}^-,t)}{L_{k+1} - L_k}, \ for\ k = 1,2,3,4, \\ \dot{\rho}_6(t) &= \frac{q(L_5^+,t) - q_{out,2}(t)}{L_6 - L_5} \end{aligned} \tag{3}$$

Here, L_i^+ denotes the downstream position whereas L_i^- denotes the upstream position. Note also that,

$$\begin{aligned} q(L_1^-,t) &= q(L_1^+,t) + q_{out,1}(t), \\ q(L_i^+,t) &= q(L_i^-,t) + u_{RM,(i-1)}(t), \end{aligned} \tag{4}$$

where $i = 2,3,4,5$. By applying the Equation (4) to (3), we have

$$\begin{aligned} \dot{\rho}_2(t) &= \frac{q(L_1^-,t) - q_{out,1}(t) - q(L_2^-,t)}{L_2 - L_1}, \\ \dot{\rho}_{k+1}(t) &= \frac{q(L_k^-,t) + u_{RM,k-1}(t) - q(L_{k+1}^-,t)}{L_{k+1} - L_k}, \\ \dot{\rho}_6(t) &= \frac{q(L_5^-,t) + u_{RM,4}(t) - q_{out,2}(t)}{L_6 - L_5} \end{aligned} \tag{5}$$

where $k = 2,3,4$. As we utilize in the present study, the state-of-art traffic simulation programs are using microscopic traffic flow models. Here, the widely known microscopic traffic model is the linear car-following model. This model is based on an elementary Newtonian physics law which is response equals to the stimulus. The car-following models adopt a speed-density relationship that is generally represented by a piecewise function

$$v(\rho) = \begin{cases} v_f, & \rho < \rho_c \\ C\Big(\dfrac{1}{\rho} - \dfrac{1}{\rho_{max}}\Big), & \rho \geq \rho_c. \end{cases}$$

where ρ_c represents the critical density and C is a sensitivity parameter. The corresponding flow-density relationship of the traffic flow can be obtained by applying $q = v\rho$

$$q(\rho) = \begin{cases} v_f\rho, & \rho < \rho_c \\ C\Big(1 - \dfrac{\rho}{\rho_{max}}\Big), & \rho \geq \rho_c \end{cases}$$

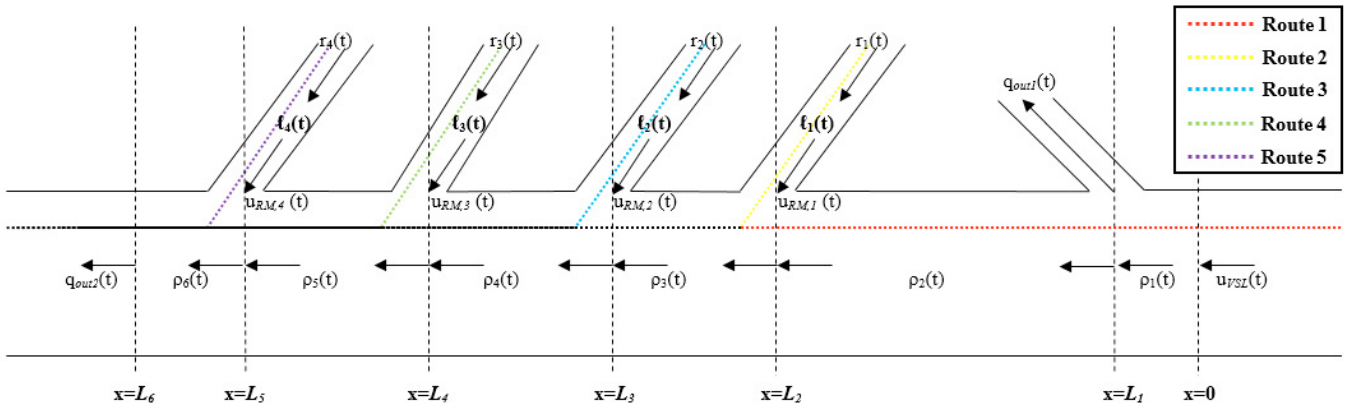

Fig. 1. The Generic Corridor.

By defining $e_i(t) = \rho_i(t) - \rho_c$ for $i = 1,2,...,6$, it is possible to express the flow dynamics for the congested state as

$$\begin{aligned} q(L_i^-,t) &= C\left(1 - \frac{e_i(t)+\rho_c}{\rho_{max}}\right), \ for\ i = 1,2,3,4,5 \\ q_{out,2}(t) &= C\left(1 - \frac{e_6(t)+\rho_c}{\rho_{max}}\right). \end{aligned} \tag{6}$$

So, the Equation (3) yields to

$$\begin{aligned} \dot{e}_1(t) &= \frac{C}{\rho_{max}L_1}e_1(t) - C\left(1 - \frac{\rho_c}{\rho_{max}}\right) \\ &\quad + \frac{1}{L_1}u_{VSL}(t), \\ \dot{e}_2(t) &= \frac{C}{\rho_{max}(L_2-L_1)}e_2(t) - \frac{C}{\rho_{max}(L_2-L_1)}e_1(t) \\ &\quad - \frac{1}{L_2-L_1}q_{out,1}(t), \\ \dot{e}_{k+1}(t) &= \frac{C}{\rho_{max}(L_{k+1}-L_k)}e_{k+1}(t) \\ &\quad - \frac{C}{\rho_{max}(L_{k+1}-L_k)}e_k(t) \\ &\quad + \frac{1}{L_{k+1}-L_k}u_{RM,(k-1)}(t), \end{aligned} \tag{7}$$

where $k = 2,3,4,5$ with the ramp dynamics

$$\dot{\ell}_i(t) = r_i(t) - u_{RM,i}(t), \ for\ i = 1,2,3,4. \tag{8}$$

So, writing (7) in a compact form yields

$$\dot{\mathbf{x}}(t) = \mathbf{A}\mathbf{x}(t) + \mathbf{B}\mathbf{u}(t) + \mathbf{w}(t). \tag{9}$$

Here,

$$\mathbf{A} = \begin{bmatrix} a_1 & 0 & 0 & 0 & 0 & 0 & 0 & 0 & 0 & 0 \\ -a_2 & a_2 & 0 & 0 & 0 & 0 & 0 & 0 & 0 & 0 \\ 0 & -a_3 & a_3 & 0 & 0 & 0 & 0 & 0 & 0 & 0 \\ 0 & 0 & -a_4 & a_4 & 0 & 0 & 0 & 0 & 0 & 0 \\ 0 & 0 & 0 & -a_5 & a_5 & 0 & 0 & 0 & 0 & 0 \\ 0 & 0 & 0 & 0 & -a_6 & a_6 & 0 & 0 & 0 & 0 \\ 0 & 0 & 0 & 0 & 0 & 0 & 0 & 0 & 0 & 0 \\ 0 & 0 & 0 & 0 & 0 & 0 & 0 & 0 & 0 & 0 \\ 0 & 0 & 0 & 0 & 0 & 0 & 0 & 0 & 0 & 0 \\ 0 & 0 & 0 & 0 & 0 & 0 & 0 & 0 & 0 & 0 \end{bmatrix},$$

$$\mathbf{B} = \begin{bmatrix} \frac{1}{L_1} & 0 & 0 & 0 & 0 \\ 0 & 0 & 0 & 0 & 0 \\ 0 & \frac{1}{(L_3-L_2)} & 0 & 0 & 0 \\ 0 & 0 & \frac{1}{(L_4-L_3)} & 0 & 0 \\ 0 & 0 & 0 & \frac{1}{(L_5-L_4)} & 0 \\ 0 & 0 & 0 & 0 & \frac{1}{(L_6-L_5)} \\ 0 & -1 & 0 & 0 & 0 \\ 0 & 0 & -1 & 0 & 0 \\ 0 & 0 & 0 & -1 & 0 \\ 0 & 0 & 0 & 0 & -1 \end{bmatrix},$$

$$\begin{aligned} \mathbf{x}(t) &= \big[e_1(t)\ \ e_2(t)\ \ e_3(t)\ \ e_4(t)\ \ e_5(t)\ \ e_6(t) \\ &\qquad \ell_1(t)\ \ \ell_2(t)\ \ \ell_3(t)\ \ \ell_4(t)\big]^T, \\ \mathbf{u}(t) &= \big[u_{VSL}(t)\ \ u_{RM,1}(t)\ \ u_{RM,2}(t)\ \ u_{RM,3}(t)\ \ u_{RM,4}(t)\big]^T, \\ \mathbf{w}(t) &= \Big[-C\left(1 - \frac{\rho_c}{\rho_{max}}\right)\ \ -\frac{1}{L_2-L_1}q_{out,1}(t)\ \ 0\ \ 0 \\ &\qquad 0\ \ 0\ \ r_1(t)\ \ r_2(t)\ \ r_3(t)\ \ r_4(t)\Big]^T, \end{aligned}$$

$$\begin{aligned} a_1 &= \frac{C}{\rho_{max}L_1},\ a_2 = \frac{C}{\rho_{max}(L_2-L_1)}, \\ a_3 &= \frac{C}{\rho_{max}(L_3-L_2)},\ a_4 = \frac{C}{\rho_{max}(L_4-L_3)}, \\ a_5 &= \frac{C}{\rho_{max}(L_5-L_4)},\ a_6 = \frac{C}{\rho_{max}(L_6-L_5)}. \end{aligned}$$

Let us define the state feedback controller as

$$\mathbf{u}(t) = \mathbf{K}\mathbf{x}(t) \tag{10}$$

and the closed-loop system (CLS) will be

$$\dot{\mathbf{x}}(t) = \mathbf{A_K}\mathbf{x}(t) + \mathbf{w}(t) \tag{11}$$

where $\mathbf{A_K} = \mathbf{A} + \mathbf{BK}$.

Remark 2. The control process is developed for the congested state of traffic flow.

4. H_∞ STATE FEEDBACK CONTROLLER

In the following, we define the H_∞ SFC to apply the combined control of freeway traffic with coordinated RM and VSL approaches. To this aim, let us define the performance index as

$$J = \int_0^\infty (\mathbf{x}^T(t)\mathbf{x}(t) - \gamma^2 \mathbf{w}^T(t)\mathbf{w}(t))dt, \tag{12}$$

where γ is a nonnegative constant. Before proceed further, let us define the H_∞ controller.

Definition 6. Given a scalar $\gamma > 0$. The state feedback controller (10) is said to be an H_∞ controller for (9), if the following two conditions hold:

(1) The CLS (11) is asymptotically stable with zero disturbance input $\mathbf{w} \equiv \mathbf{0}$.
(2) There exists a Lyapunov function of class C^1 satisfying $\dot{V} < \gamma^2 \mathbf{w}^T(t)\mathbf{w}(t) - \mathbf{x}^T(t)\mathbf{x}(t)$ for every non-zero $\mathbf{w} \in L_2$ on $[0,\infty)$.

Theorem 7. The system (9) is asymptotically stable and the H_∞ performance bound constraint $J < 0$ holds for every $\gamma > 0$, if there exists matrices $\mathbf{P} > 0$ and $\mathbf{Y}$ satisfying

$$\begin{bmatrix} \Omega_{11} & \mathbf{I} & \mathbf{P} \\ * & -\gamma^2\mathbf{I} & 0 \\ * & * & -\mathbf{I} \end{bmatrix} < 0. \tag{13}$$

where $\Omega_{11} = \mathbf{AP} + \mathbf{PA}^T + \mathbf{BY} + \mathbf{Y}^T\mathbf{B}^T$. The gain matrix is perceived as $\mathbf{K} = \mathbf{YP}^{-1}$.

Proof: Let us consider the Lyapunov functional $V(\mathbf{x}(t)) = \mathbf{x}^T(t)\mathbf{P}^{-1}\mathbf{x}(t)$. So, the Hamiltonian will be

$$\begin{aligned} H(\mathbf{x}(t),\mathbf{w}(t),t) =& \dot{V}(\mathbf{x}(t)) + \mathbf{x}^T(t)\mathbf{x}(t) - \gamma^2\mathbf{w}^T(t)\mathbf{w}^T(t) \\ =& 2\mathbf{x}^T(t)\mathbf{P}^{-1}\dot{\mathbf{x}}(t) + \mathbf{x}^T(t)\mathbf{x}(t) - \gamma^2\mathbf{w}^T(t)\mathbf{w}^T(t) \\ =& \begin{bmatrix} \mathbf{x}(t) \\ \mathbf{w}(t) \end{bmatrix}^T \begin{bmatrix} \overline{\Omega}_{11} & \mathbf{P}^{-1} \\ * & -\gamma^2\mathbf{I} \end{bmatrix} \begin{bmatrix} \mathbf{x}(t) \\ \mathbf{w}(t) \end{bmatrix} \end{aligned}$$

where $\overline{\Omega}_{11} = \mathbf{A_K}^T\mathbf{P}^{-1} + \mathbf{P}^{-1}\mathbf{A_K} + \mathbf{I}$. By state transformation, one can write

$$\begin{aligned} &H(\mathbf{x}(t),\mathbf{w}(t),t) \\ &= \begin{bmatrix} \mathbf{x}(t) \\ \mathbf{w}(t) \end{bmatrix}^T \begin{bmatrix} \mathbf{P}^{-1} \\ \mathbf{I} \end{bmatrix}^T \begin{bmatrix} \Omega_{11} + \mathbf{P}^T\mathbf{P} & \mathbf{I} \\ * & -\gamma^2\mathbf{I} \end{bmatrix} \begin{bmatrix} \mathbf{P}^{-1} \\ \mathbf{I} \end{bmatrix} \begin{bmatrix} \mathbf{x}(t) \\ \mathbf{w}(t) \end{bmatrix}. \end{aligned}$$

By using Lemma 5, $H(\mathbf{x}(t),\mathbf{w}(t),t) < 0$ holds if (13) is satisfied.

5. SIMULATION SETUP

In this section, we first present our framework in order to implement the H_∞ SFC into VISSIM through MATLAB. Following the framework, the simulation process is decomposed into the following stages:

(1) Field data are collected and network characteristics are determined from the study field.
(2) Network parameters, vehicle inputs, vehicle routes, simulation settings, signal controllers, signal groups and detectors are determined through VISSIM whereas the system matrices are calculated through MATLAB.
(3) Occupancy values of each segment of the road and queue lengths of each on-ramps are measured for each simulation cycle. Then, occupancy values are converted into density and then into error terms to form the state vector.
(4) Meanwhile, (13) is solved via LMI Toolbox of MATLAB to calculate the feedback gain.
(5) Once the state vector and feedback gain is evaluated, the flow values are obtained to decide the green time value of the current cycle and the VSL value to be shown.

In order to analyze the peak-hour effect and demonstrate the control performance in varying flow conditions, the duration of simulation is set to run for three hours. The simulations are executed for both "No Control" and H_∞ SFC cases using a personal computer with an i7 CPU with 3.0 GHz processor and 8 GB RAM. The critical parameters of traffic flow are set to $v_f = 120\ km \cdot h^{-1}$, $\rho_c = 80\ veh \cdot km^{-1} \cdot lane^{-1}$ and $\rho_{max} = 200\ veh \cdot km^{-1} \cdot lane^{-1}$. The cycle time and the minimum green time for RM are chosen as 15 *sec* and 5 *sec*, respectively. Note that the sensitivity constant will be

$$C = \frac{v_f}{\frac{1}{\rho_c} - \frac{1}{\rho_{max}}}.$$

In order to apply Theorem 7, we choose the H_∞ gain as $\gamma^2 = 1.5$. Rest of the simulation parameters are given in Table 1.

Table 1. Simulation Parameters

Parameter	Values
Standstill Distance	1.50 m
Headway Time	2.00 s
Following Variation	3.50 m
Threshold for Entering	-8.00 s
Following Threshold (-)	-0.35 $m \cdot s^{-1}$
Following Threshold (+)	0.40 $m \cdot s^{-1}$
Speed Dependency of Oscillation	11.00 $(m \cdot s)^{-1}$
Oscillation Acceleration	0.25 $m \cdot s^{-2}$
Standstill Acceleration	3.50 $m \cdot s^{-2}$
Acceleration with 80 $km \cdot h^{-1}$	1.50 $m \cdot s^{-2}$

The test corridor is a piece of the D-100 freeway on the European side of Istanbul with the segment characteristics given in Table 2.

Table 2. Segment Properties

Segment No	# of Lanes	Length (km)	Density
1	4	4.29	$\rho_1(t)$
2	3	0.79	$\rho_2(t)$
3	3	0.96	$\rho_3(t)$
4	4	0.67	$\rho_4(t)$
5	4	0.03	$\rho_5(t)$
6	4	1.14	$\rho_6(t)$

Field data are obtained from successive microwave sensor units located on the freeway segment to our interest. The measurements are aggregated in 2 mins interval and are used for the calibration process.

In order to apply RM, the green time values are evaluated by calculating $u_{RM,i}(k)$ for each cycle k with (10). Then, the green time $GT_i(k)$ to be applied is determined as

$$GT_i(k) = \begin{cases} MGT, & u_{RM,i}(k) < MFR \\ \dfrac{u_{RM,i}(k)}{u_{sat}} \cdot CT, & MFR \leq u_{RM,i}(k) \leq u_{sat} \\ CT, & u_{RM,i}(k) > u_{sat} \end{cases}$$

where

- MGT is the minimum green time,
- $MFR = \frac{u_{sat} \cdot MGT}{CT}$ is the minimum flow rate,
- CT is the cycle time,
- u_{sat} is the saturated flow.

In order to adjust the green time in each cycle, $GT_i(k)$ is defined as a piecewise function. The green time in each cycle is bounded above by the cycle time and below by the predetermined minimum green time. In case of high congestion, the minimum green time constraint will be considered. In the absence of such kind of a constraint, the corresponding ramp signal would be adjusted to red during the whole cycle time. Between the minimum green time and the cycle time, $GT_i(k)$ takes the value $\frac{u_{RM,i}(k)}{u_{sat}} \cdot CT$ which is the equivalent value of $u_{RM,i}(k)$ in the cycle time.

To apply VSL, the desired flow values $u_{VSL}(k)$ are calculated for every cycle k. Then, it is converted to desired speed values $v_{VSL}(k)$ by using the speed-flow relationship of car-following model. The speed values to be reflected $v_{refl}(k)$ are calculated as

$$v_{refl}(k) = \begin{cases} v_{min}, & v_{VSL}(k) < v_{min} \\ 10 \cdot \lfloor v_{VSL}(k)/10 \rfloor, & v_{min} \leq v_{VSL}(k) \leq v_{max} \\ v_{max}, & v_{VSL}(k) > v_{max} \end{cases}$$

where $\lfloor \cdot \rfloor$ function rounds its argument to the next smaller integer, $v_{min} = 50\ km \cdot h^{-1}$ is the minimum speed to be shown, $v_{max} = 120\ km \cdot h^{-1}$ is the maximum speed to be shown. As in the determination of green time in each cycle, the speed values to be reflected are also defined by a piecewise function. If $v_{VSL}(k)$ is in the range between the predetermined minimum and maximum speed values, then it is floored to the closest multiple of 10. For instance, in case that $v_{VSL}(k)$ is calculated as 67 $km \cdot h^{-1}$, the speed limit $v_{refl}(k)$ will be 60 $km \cdot h^{-1}$.

6. RESULTS AND DISCUSSION

This research provides an overview of applications of RM and VSL algorithms on a real network located in Istanbul. As far as it is seen from Table 3 and 4, it can be seen that coordinated RM and VSL using H_∞ SFC gives better results for minimizing the average densities of mainflow segments in contrast to "No Control" case without having a dramatic increase in the average queue lengths of the corresponding ramps.

Table 3. Average Densities of Mainflow Segments (in $veh \cdot km^{-1}$)

	# of Lanes	No Control	H_∞ SFC
$\rho_1(t)$	4	327.42	210.28
$\rho_2(t)$	3	274.01	203.37
$\rho_3(t)$	3	214.65	156.81
$\rho_4(t)$	4	259.89	199.18
$\rho_5(t)$	4	105.27	92.15
$\rho_6(t)$	4	75.49	91.88

The most significant change can be observed for $\rho_1(t)$ which represents the density of Segment 1. The major reason for that is the segment length plays an important role to calculate the density. Moreover, it should be pointed out that the H_∞ SFC case gives low-density values despite the fact that the ramps have longer queue lengths.

Table 4. Average Queue Length of the Corresponding Ramps (in m)

	No Control	H_∞ SFC
$\ell_1(t)$	187.99	191.26
$\ell_2(t)$	175.83	181.44
$\ell_3(t)$	182.42	188.96
$\ell_4(t)$	172.73	183.36

The occupancy profiles under "No Control" and H_∞ SFC cases for the mainline are presented in Figure 2.

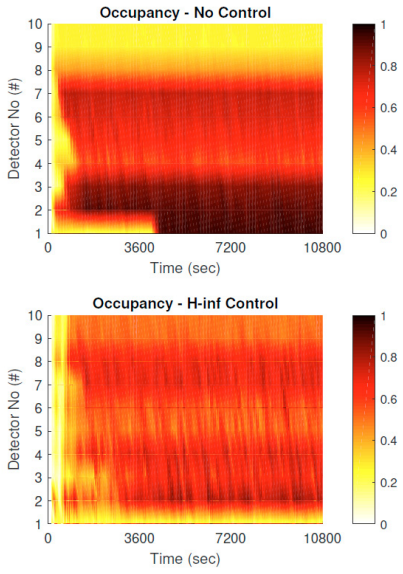

Fig. 2. Occupancy Maps of "No Control" and H_∞ SFC Cases.

It should be noted that the occupancy values are kept under the critical value of 0.8 on the mainline during the simulation.

For the analysis of the total outflow performance of the network, the total throughput of the system in a two minute period is collected. As seen in Figure 3, the H_∞ SFC causes a fluctuation in the as an early effect, however after that the H_∞ SFC outperforms the "No Control" case and a 20.37 % increase in total throughput is achieved with the consideration of the early effect, but after that the average increase of the total throughput is reached at 22.98 %.

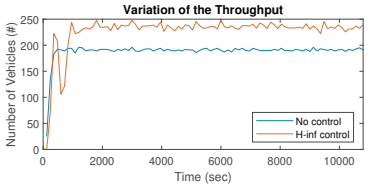

Fig. 3. Throughput of System.

7. CONCLUSIONS

Aiming to enhance the performance of the mainstream traffic flow with a tolerable queue accumulation on on-ramps, we proposed the integrated freeway control approach by coordinating the applications of RM and VSL based on H_∞ SFC. Based on

the test results from microscopic simulations, the mainstream traffic flow was kept under a defined critical density while the queue accumulation on the ramps were retarded. Future directions of our research include alternating the effects of driver behavior on simulation adopting different car-following models and adapting our control strategy to different future mobility applications.

ACKNOWLEDGEMENT

The work summarized in this paper is supported in part by The Scientific & Technological Research Council of Turkey (TÜBİTAK) under the project with no. 120M576. First author would like to express his acknowledgement to PTV AG by providing the license of the microscopic traffic simulator VISSIM.

REFERENCES

Boyd, S. and Vandenberghe, L. (2004). *Convex Optimization*. Cambridge University Press.

Caligaris, C., Sacone, S., and Siri, S. (2007). Optimal ramp metering and variable speed signs for multiclass freeway traffic. In *2007 European Control Conference (ECC)*, 1780–1785. IEEE.

Carlson, R.C., Papamichail, I., and Papageorgiou, M. (2011). Local feedback-based mainstream traffic flow control on motorways using variable speed limits. *IEEE Transactions on Intelligent Transportation Systems*, 12(4), 1261–1276.

Carlson, R.C., Papamichail, I., and Papageorgiou, M. (2014). Integrated feedback ramp metering and mainstream traffic flow control on motorways using variable speed limits. *Transportation research part C: Emerging technologies*, 46, 209–221.

Celikoglu, H.B. and Dell'Orco, M. (2008). A dynamic model for acceleration behaviour description in congested traffic. In *2008 11th International IEEE Conference on Intelligent Transportation Systems*, 986–991. IEEE.

Csikós, A., Varga, I., and Hangos, K.M. (2013). Freeway shockwave control using ramp metering and variable speed limits. In *21st Mediterranean Conference on Control and Automation*, 1569–1574. IEEE.

Fountoulakis, M., Bekiaris-Liberis, N., Roncoli, C., Papamichail, I., and Papageorgiou, M. (2017). Highway traffic state estimation with mixed connected and conventional vehicles: Microscopic simulation-based testing. *Transportation Research Part C: Emerging Technologies*, 78, 13–33.

Gomes, G. and Horowitz, R. (2006). Optimal freeway ramp metering using the asymmetric cell transmission model. *Transportation Research Part C: Emerging Technologies*, 14(4), 244–262.

Hajiahmadi, M., De Schutter, B., and Hellendoorn, H. (2013). Robust h_∞ control for switched nonlinear systems with application to high-level urban traffic control. In *52nd IEEE Conference on Decision and Control*, 899–904. IEEE.

Hajiahmadi, M., De Schutter, B., and Hellendoorn, H. (2016). Robust h_∞ switching control techniques for switched nonlinear systems with application to urban traffic control. *International Journal of Robust and Nonlinear Control*, 26(6), 1286–1306.

Iordanidou, G.R., Roncoli, C., Papamichail, I., and Papageorgiou, M. (2015). Feedback-based mainstream traffic flow control for multiple bottlenecks on motorways. *IEEE Transactions on Intelligent Transportation Systems*, 16(2), 610–621.

Kachroo, P. and Ozbay, K. (2003). *Feedback Ramp Metering in Intelligent Transportation Systems*. Kluwer Academic/Plenum Publishers, New York.

Khalil, H.K. (2002). *Nonlinear Systems*, volume 3. Prentice hall Upper Saddle River, NJ.

Lemarchand, A., Koenig, D., and Martinez, J.J. (2011). Smooth switching H_∞ PI controller for local traffic on-ramp metering, an LMI approach. *IFAC Proceedings Volumes*, 44(1), 13882–13887.

Lu, X.Y., Qiu, T.Z., Varaiya, P., Horowitz, R., and Shladover, S.E. (2010a). Combining variable speed limits with ramp metering for freeway traffic control. In *Proceedings of the 2010 american control conference*, 2266–2271. IEEE.

Lu, X.Y., Varaiya, P., Horowitz, R., Su, D., and Shladover, S.E. (2010b). A new approach for combined freeway variable speed limits and coordinated ramp metering. In *13th International IEEE Conference on Intelligent Transportation Systems*, 491–498. IEEE.

Luspay, T., Csikós, A., Péni, T., Varga, I., and Kulcsár, B. (2017). Ramp metering for flow maximisation and emission reduction–a set-based multi-objective design approach. *Transportation Research Procedia*, 27, 937–944.

Mohajerpoor, R., Saberi, M., Vu, H.L., Garoni, T.M., and Ramezani, M. (2020). H_∞ robust perimeter flow control in urban networks with partial information feedback. *Transportation Research Part B: Methodological*, 137, 47–73.

Müller, E.R., Carlson, R.C., Kraus, W., and Papageorgiou, M. (2015). Microsimulation analysis of practical aspects of traffic control with variable speed limits. *IEEE Transactions on Intelligent Transportation Systems*, 16(1), 512–523.

Pasquale, C., Sacone, S., and Siri, S. (2014). Ramp metering control for two vehicle classes to reduce traffic emissions in freeway systems. In *2014 European Control Conference (ECC)*, 2588–2593. IEEE.

Roncoli, C., Papageorgiou, M., and Papamichail, I. (2015a). Traffic flow optimisation in presence of vehicle automation and communication systems–part i: A first-order multi-lane model for motorway traffic. *Transportation Research Part C: Emerging Technologies*, 57, 241–259.

Roncoli, C., Papageorgiou, M., and Papamichail, I. (2015b). Traffic flow optimisation in presence of vehicle automation and communication systems–part ii: Optimal control for multi-lane motorways. *Transportation Research Part C: Emerging Technologies*, 57, 260–275.

Sadat, M. and Celikoglu, H.B. (2017). Simulation-based variable speed limit systems modelling: an overview and a case study on istanbul freeways. *Transportation research procedia*, 22, 607–614.

Silgu, M.A., Muderrisoglu, K., Unsal, A.H., and Celikoglu, H.B. (2018). Approximation of emission for heavy duty trucks in city traffic. In *2018 IEEE International Conference on Vehicular Electronics and Safety (ICVES)*, 1–4. IEEE.

Zhang, Y. and Ioannou, P.A. (2018a). Integrated control of highway traffic flow. *Journal of Control and Decision*, 5(1), 19–41.

Zhang, Y. and Ioannou, P.A. (2018b). Stability analysis and variable speed limit control of a traffic flow model. *Transportation Research Part B: Methodological*, 118, 31–65.